Available online at www.sciencedirect.com
ScienceDirect
Bioorganic & Medicinal Chemistry Letters
Bioorganic & Medicinal Chemistry Letters 16 (2006) 5066–5072

Solid-phase synthesis and structure–activity relationships of novel biarylethers as melanin-concentrating hormone receptor-1 antagonists

Vu Ma,[a,*] Anthony W. Bannon,[d] Jamie Baumgartner,[e] Clarence Hale,[b] Faye Hsieh,[c] Christopher Hulme,[f] Kirk Rorrer,[e] John Salon,[b] Carlo van Staden[b] and Paul Tempest[g]

[a]*Chemistry Research and Discovery, Amgen Inc., One Amgen Center Drive, Thousand Oaks, CA 91320, USA*
[b]*Department of Metabolic Disorders, Amgen Inc., One Amgen Center Drive, Thousand Oaks, CA 91320, USA*
[c]*Department of Pharmacokinetics and Drug Metabolism, Amgen Inc., One Amgen Center Drive, Thousand Oaks, CA 91320, USA*
[d]*Icagen Inc., 4222 Emperor Blvd, Suite 350, Durham, NC 27703, USA*
[e]*MDS Pharma Services, 22011 30th Dr SE, Bothell, WA 98021, USA*
[f]*Eli Lilly and Company, 9560 Copley Drive, Indianapolis, IN 46260, USA*
[g]*Merck Research Labs, 33 Avenue Louis Pasteur, Boston, MA 02115, USA*

Received 21 June 2006; revised 11 July 2006; accepted 12 July 2006
Available online 1 August 2006

Abstract—Melanin-concentrating hormone (MCH) is a cyclic 19 amino acid orexigenic neuropeptide. The action of MCH on feeding is thought to involve the activation of its respective G protein-coupled receptor MCH-R1. Consequently, antagonists that block MCH regulated MCH-R1 activity may provide a viable approach to the treatment of diet-induced obesity. This communication reports the discovery of a novel MCH-R1 receptor antagonist, the biarylether **7**, identified through high throughput screening. The solid-phase synthesis and structure–activity relationship of related analogs is described.

The prevalence of obesity and obesity related fatality is on the increase in the industrialized world. Today in the United States, nearly two-thirds of adults are obese or overweight and the problem is anticipated to be a major contributor to a potential decline in life expectancy in the 21st century.[1] Unfortunately, the usefulness of currently available drugs for the treatment of obesity has proven disappointing, due in part to poor efficacy and off-target side effects.[2]

Accordingly, the search for drugs and drug targets that selectively modulate physiological systems directly involved in feeding and metabolism has become a pressing concern in the pharmaceutical sector. Several lines of evidence have implicated the melanin-concentrating hormone (MCH) system as a pivotal regulator of food intake and energy homeostasis.[3] First, both genetically obese mice and mice that have been fasted display up-regulated levels of MCH precursor messenger RNA in the lateral hypothalamus, a key area of the brain regulating feeding behavior.[4] Second, injection of the MCH peptide itself directly into the brain is sufficient to stimulate feeding in rats.[5] Finally, knock-out mice that lack MCH eat less and are lean, while transgenic mice that overexpress MCH develop insulin resistance and become obese.[6,7]

The MCH transmitter system includes at least two subtypes of G protein-coupled receptors (GPCRs), designated MCH-R1 and MCH-R2.[8,9] While the differential role of these subtypes in neurophysiology and behavior has not been defined, the evidence at hand suggests that MCH-R1 plays a more prominent role in the regulation of diet-induced obesity in humans.[10–12] Several structurally distinct MCH-R1 antagonists have been reported in Figure 1 (**1**[13], **2**[14], **3**[15], **4**[16], **5**[17], **6**[18,19], **7**[20], and **8**[21]).

Recently, Schering-Plough reported urea **7** (Fig. 1) exhibited a significant reduction in food intake and weight gain, and significantly reduced cumulative food

Keywords: Biarylethers; MCH-R1 antagonists.
* Corresponding author. Tel.: +1 805 447 8394; e-mail: vma@amgen.com

0960-894X/$ - see front matter © 2006 Elsevier Ltd. All rights reserved.
doi:10.1016/j.bmcl.2006.07.040

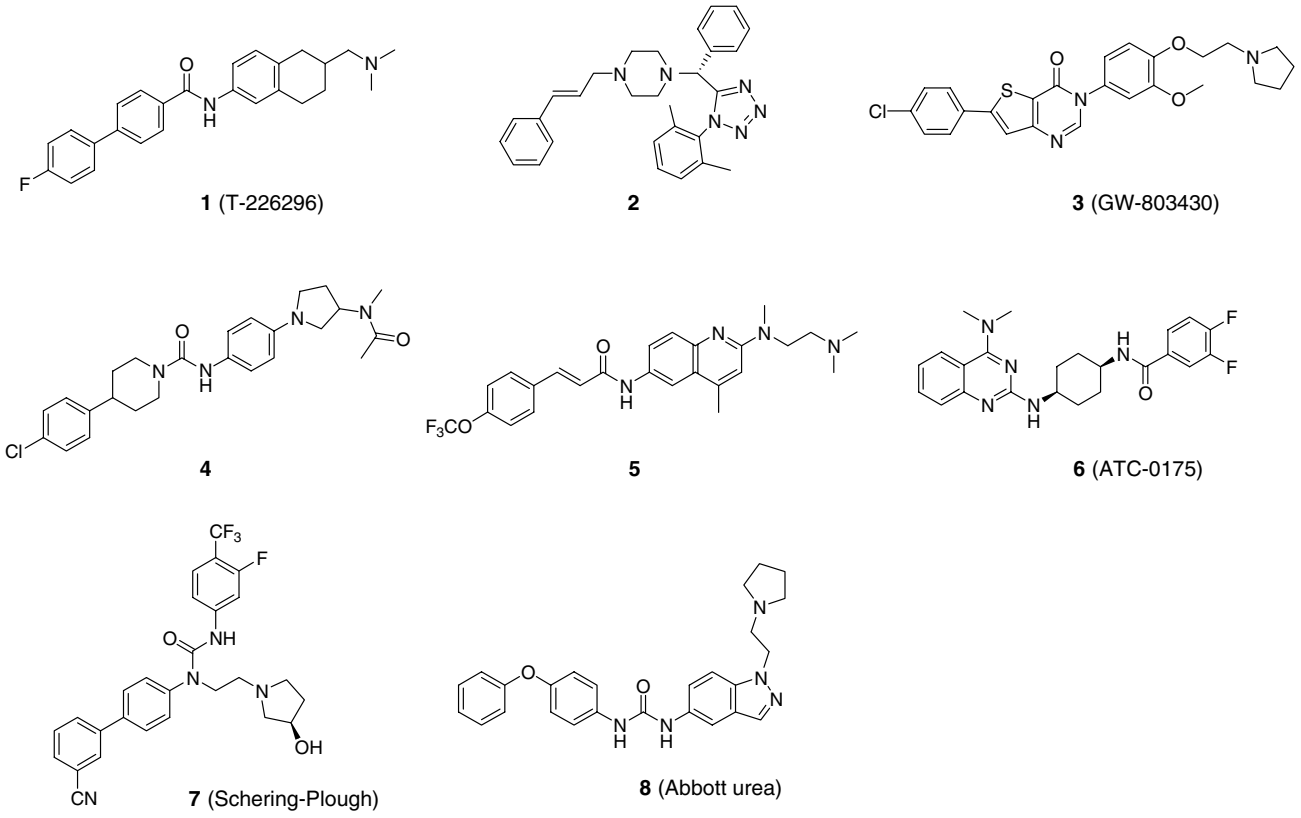

Figure 1. Reported MCH-R1 antagonists.

intake by day 28 at 30 mg/kg, oral dosing in diet-induced obese (DIO) mouse model. In addition, Abbott reported urea **8** (Fig. 1) exhibited a significant reduction in food intake and a significant cumulative reduction by day 14 at 100 mg/kg, oral dosing in DIO mouse model. Herein we report the structure–activity relationships (SAR) and pharmacokinetic properties of biarylether-containing MCH-R1 antagonists prepared by an efficient solid-phase synthesis.

The Amgen corporate collection was evaluated in a high-throughput scintillation proximity assay (HTSPA) for binding versus rat MCH-R1 at a single 10 μM dose. Validated hits were further screened for binding to both human, and mouse MCH-R1.[22] Select compounds were assayed for functional activity using a FLIPR® protocol measuring the MCH-R1 induced mobilization of intracellular Ca^{2+}.[23] Several sub-micromolar compounds emerged from the screening and validation process, including compound **9** (Fig. 2) with an IC_{50} (rMCH-R1) = 250 ± 70 nM. Compound **9** possesses three readily modified groups, R^1, R^2, and R^3 (structure **16**, Scheme 1), amenable to rapid analoging via solid-phase synthesis.

Solid-phase synthesis of the series is described generically in Scheme 1.[24] Commercially available 4-formyl-3-methoxyphenoxy-polystyrene resin (**10**) was reductively aminated to introduce R^3 (**11**). Acylation with 4-fluoro-3-nitrobenzoic acid afforded **12**, which upon treatment with the desired phenol, thiophenol or aniline in the presence of a base provided **13**. Nitro group reduction with tin (II) chloride dihydrate gave the amine, **14**, which was then converted to the amide, carbamate or urea (**15**). Cleavage from the resin with trifluoroacetic acid followed by purification by silica gel chromatography provided the desired products (**16**). Unless otherwise noted, purity of compounds **17**–**39** was >95% as determined by reversed-phase HPLC.

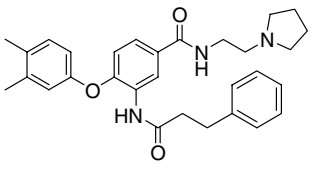

9

IC_{50} (rMCH-R1) = 250 ± 70.0 nM
IC_{50} (hMCH-R1) = 330 ± 160 nM
IC_{50} (mMCH-R1) = 610 ± 130 nM

Figure 2. Compound **9**, screening hit from HT-SPA assay.

The in vitro IC_{50} data from the SPA assay at rat, human, and mouse MCH receptor-1 (rMCH-R1, hMCH-R1, and mMCH-R1, respectively) for compounds **17-33** compared to compound **9** are given in Table 1. Unless otherwise noted, IC_{50} values are the average of at least two separate experiments and are reported with the standard error of the mean (SEM).

Based on the results from Table 1, several observations were made. For example, a tertiary amine (e.g., **9**) was

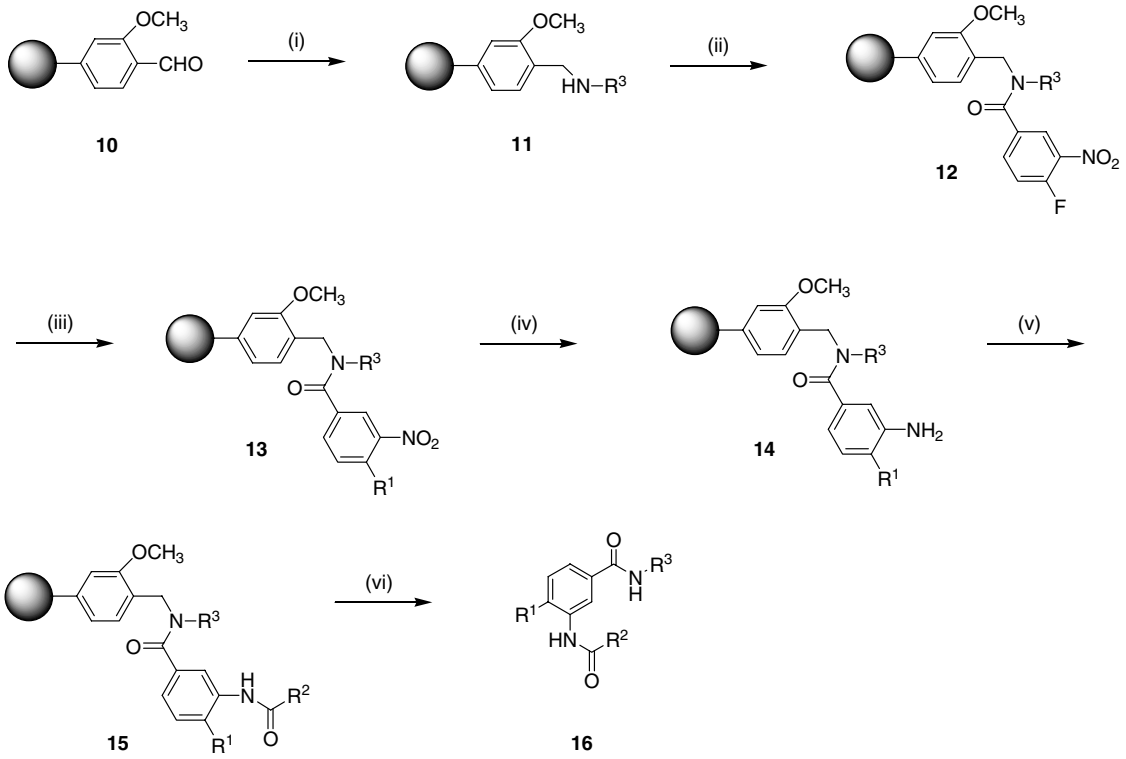

Scheme 1. Synthesis of compounds **9**, **17-39**. (i) R^3NH_2, $Na(OAc)_3BH$, dichloroethane; (ii) 4-fluoro-3-nitrobenzoic acid, HOBT, DIC, DMF; (iii) ArOH or ArSH or $ArNH_2$, DBU, DMF; (iv) $SnCl_2 \cdot 2H_2O$, DMF; (v) acid chloride or isocyanate or chloroformate, pyridine, dichloromethane; (vi) trifluoroacetic acid, dichloromethane.

preferred over a primary amine (e.g., **17**) at the terminus of R^3. The presence of a tertiary amine is common to MCH-R1 antagonists and accounts for a key salt bridge interaction with the receptor.[25] Replacement of the oxygen linker at R^1 with either sulfur (e.g., **18**) or nitrogen (e.g., **19**) resulted in a significant reduction in potency. Replacement of 3,4-dimethyl phenyl at R^1 with naphthyl had little impact on activity (compare compound **9** with **20**). Note that the biaryl ether motif is common to multiple GPCR receptor ligands.[26,27] Activity was not impacted significantly when the phenethyl amide at R^2 was replaced with a *trans*-cinnamide (compound **9** vs. **21**). The *trans*-cyclopropane (**22**) was also tolerated. Truncation of the phenethyl at R^2 to benzyl, ethyl, and methyl (compounds **23**, **24**, and **25**, respectively) resulted in a reduction in activity. While the phenyl carbamate (**26**) was less active than screening hit **9**, the analogous phenyl urea (**27**) showed an improvement in potency up to 100-fold. Compound **27** possessed single digit nM activities for all 3 receptor types (rat, human, and mouse). Further examination of the ureas showed that the *N*-methyl (**28**) and pyridyl (**29**) analogs suffered from a significant reduction in activity. The reduction in potency going from phenyl urea **27** to phenyl carbamate **26**, *N*-methyl phenyl urea **28** or 2-aminopyridyl urea **29** suggests that the urea NH is involved in a key hydrogen-bonding interaction with the receptor. Certain substituents on the urea phenyl, for example *ortho*-chloro (**30**), and *para*-bromo (**31**), were tolerated and resulted in low nanomolar potency for all three species. More bulky substituents such as *para*-phenyl (**32**) and *para*-phenyloxy (**33**) caused a decrease in potency relative to **27**.

Compound **27** was further profiled in vitro and a summary of the potency and functional activity for the three species is given in Table 2. Compound **27** was potent in the functional assay (FLIPR® Ca^{2+} release: K_i (hMCH-R1) = 13 ± 5 nM; K_i (rMCH-R1) = 13 ± 5 nM; K_i (mMCH-R1) = 14 ± 4 nM). Mechanisms of ligand interaction with MCH-R1 as determined by Schild analysis[28] showed that compound **27** was a reversible, competitive antagonist (pA2 = 8; equivalent to K_d = 10 nM).

The pharmacokinetic profile of compound **27** was then examined. A high rate of clearance was observed in vitro in rat liver microsomes (RLM CL = 703 μL/min/mg)[29] and, consistent with this result, the compound was cleared very rapidly in vivo (iv 2 mg/kg in Sprague–Dawley rats; CL = >10,000 mL/kg/h; $t_{1/2}$ = 0.7 h).[30] In addition, brain penetration in rats was limited, with 30 min peak levels of less than 40 ng/g (based on whole brain homogenate), raising concerns that sufficient exposure would not be achieved when dosing iv in the efficacy model. Phase I metabolite identification studies in rat liver microsomes suggested multiple sites of oxidation (Fig. 3) based on mass fragments observed by LC/MS/MS. A series of closely related analogs was designed to prevent metabolic oxidation (Table 3). Low nanomolar potency was maintained and a clear trend was observed in the microsomal clearance data, confirming that the methyl groups on R^1 and aryl *meta*-position on R^2 are major sites of phase I metabolism. Introducing a single fluorine to the aromatic ring in the *meta*-position at R^2 (compare compound **27** to **34**)

Table 1. Inhibition (IC_{50}) of MCH binding to rat, human, and mouse MCH-R1 in the SPA assay

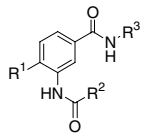

Compound	R^1	R^2	R^3	IC_{50} rMCH-R1 (nM)	IC_{50} hMCH-R1 (nM)	IC_{50} mMCH-R1 (nM)
9	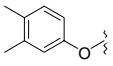	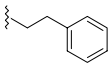	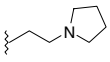	250 ± 70.0	330 ± 160	610 ± 130
17	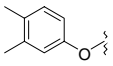	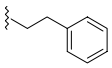	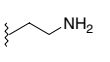	>1000	>1000	>1000
18[a]	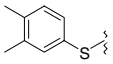	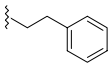	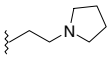	>1000	>1000	>1000
19[b]	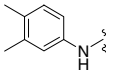	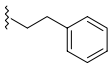	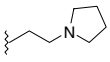	>1000	>1000	>1000
20	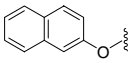	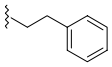	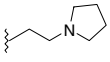	540 ± 230	380 ± 160	340 ± 10.0
21	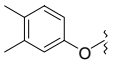	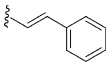	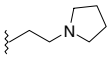	170 ± 60.0	540 ± 230	230 ± 120
22	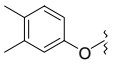	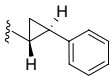	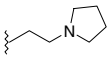	320 ± 160	170 ± 70.0	n.d.[c]
23	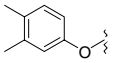		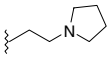	>1000	>1000	>1000
24	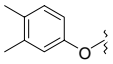		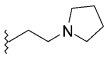	>1000	>1000	>1000
25	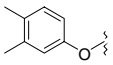		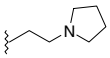	>1000	>1000	>1000
26[d]	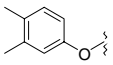		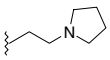	>1000	>1000	>1000
27	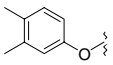		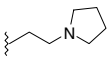	3.00 ± 1.00	7.00 ± 3.00	5.00 ± 2.00
28	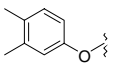		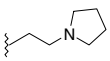	>1000	>1000	>1000
29				>1000	>1000	>1000
30				14.0 ± 5.00	15.0 ± 4.00	7.00 ± 1.00
31				5.00 ± 1.00	11.0 ± 6.00	28.0 ± 9.00
32				260 ± 80.0	140 ± 50.0	400 ± 70.0
33				610 ± 150	340 ± 100	460 ± 60.0

[a] LC purity = 93% (215 nm); 92% (254 nm).
[b] LC purity = 85% (215 nm); 85% (254 nm).
[c] n.d. = not determined.
[d] LC purity = 92% (215 nm); 92% (254 nm).

Table 2. Compound **27** in vitro binding potency versus functional activity

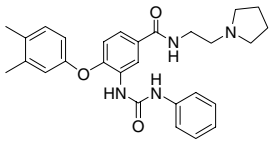

Assay	rMCH-R1	hMCH-R1	mMCH-R1
SPA (binding, K_i)	2.00 ± 0.67 nM	4.70 ± 2.00 nM	3.30 ± 1.30 nM
FLPR® (functional, K_i)	13.0 ± 5.00 nM	13.0 ± 5.00 nM	14.0 ± 4.00 nM

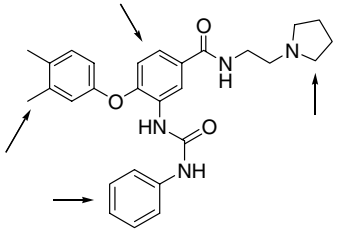

Figure 3. Sites of phase I metabolism of compound **27**.[29]

reduced microsomal clearance over two-fold (RLM CL = 264 μL/min/mg for **34** vs. 703 μL/min/mg for **27**). Less of an impact on clearance was observed for the analogous mono-methylated analogs **35** and **36** (RLM CL = 469 and 692 μL/min/mg, respectively). Replacing one or both of the methyl groups in **34** with fluorine (e.g., **37** and **38**) was tolerated in terms of potency, but did not result in a significant improvement in clearance over **34**. Compound **39**, possessing a single fluorine in the *meta*-position of each of the aromatic rings (R^1 and R^2), had the lowest in vitro clearance of the series (RLM CL = 196 μL/min/mg) and was further profiled in vivo.

Upon iv dosing in the rat (Table 4), compound **39** showed an improvement over compound **27** in terminal half-life (3.9 h), clearance (5600 mL/kg/h), and volume of distribution (23000 mL/kg). Brain levels, however, remained low (46 ng/g at 30 min, based on whole brain homogenate). When dosed orally (30 mg/kg in 1% HPMC/1% Tween 80), with plasma and brain levels monitored over eight hours, compound **39** was below the limit of quantification.

In summary, the collective data for this novel series of MCH-R1 antagonists suggest that, although possessing

Table 3. In vitro potency and rat liver microsomal (RLM) clearance for compound **27** compared to compounds **34–39**

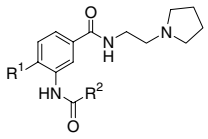

Compound	R^1	R^2	IC_{50} rMCH-R1 (nM)	IC_{50} hMCH-R1 (nM)	RLM CL (μL/min/mg)
27	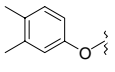		3.00 ± 1.00	7.00 ± 3.00	703
34	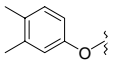	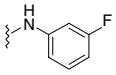	3.00 ± 1.00	2.00 ± 1.00	264
35	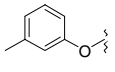	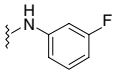	7.00 ± 0.10	2.00 ± 1.00	469
36	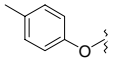	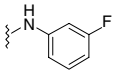	33.0 ± 19.0	2.00 ± 0.50	692
37	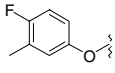	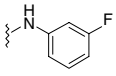	6.00 ± 3.00	0.10[a]	258
38	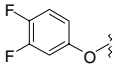	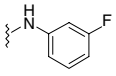	28.0 ± 9.00	1.40[a]	393
39	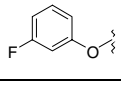	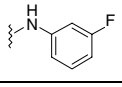	40.0 ± 26.0	9.00 ± 5.00	196

[a] IC_{50} value based on $n = 1$ experiment.

Table 4. Comparison of pharmacokinetic profile for compounds **27** and **39**

Compound	In vitro RLM CL (μL/min/mg)	In vivo CL[a] (mL/kg/h)	$t_{1/2}$ (h)	V_{ss} (mL/kg)	Brain levels[b] (ng/g)
27	703.00	>10000	0.7000	9800.0	31.000
39	196.00	5600.0	3.9000	23000	46.000

[a] 2 mg/kg in DMSO dosed in male Sprague–Dawley rats.
[b] Based on brain homogenate taken at 0.5 h post-dose.

both excellent in vitro binding and functional activity, these compounds suffer from high clearance and poor blood–brain barrier penetration. Sites of metabolism were identified and blocked to reduce clearance rates. Current efforts are focused on achieving sufficient exposure for in vivo efficacy studies.

Acknowledgment

The authors thank our colleague, Liz Doherty, for her assistance in manuscript preparation and her helpful suggestions.

References and notes

1. Olshansky, S. J.; Passaro, J. D.; Hershow, R. C.; Layden, J.; Carnes, B. A.; Brody, J.; Hayflick, L.; Butler, R. N.; Allison, D. B.; Ludwig, D. S. *N. Engl. J. Med.* **2005**, *352*, 1138.
2. Gura, T. *Science* **2003**, *299*, 849.
3. Qu, D.; Ludwig, D. S.; Gammeltoft, S.; Piper, M.; Pelleymounter, M. A.; Cullen, M. J.; Mathes, W. F.; Przypek, J.; Kanarek, R.; Maratos-Filer, E. *Nature* **1996**, *380*, 243.
4. Hervieu, G. J.; Cluderay, J. E.; Harrison, D.; Meakin, J.; Maycox, P.; Nasir, S.; Leslie, R. A. *Eu. J. Neuroscience* **2000**, *12*, 1194.
5. Marsh, D. J.; Weingarth, D. T.; Novi, D. E.; Chen, H. Y.; Trumbauer, M. E.; Chen, A. S.; Guan, X.-M.; Jiang, M. M.; Feng, Y.; Camacho, R. E.; Shen, Z.; Frazier, E. G.; Yu, H.; Metzger, J. M.; Kuca, S. J.; Shearman, L. P.; Gopal-Truter, S.; MacNeil, D. J.; Strack, A. M.; MacIntyre, D. E.; Van der Ploeg, H. T.; Qian, S. *Proc. Natl. Acad. Sci.* **2002**, *99*, 3240.
6. Shimada, M.; Tritos, N. A.; Lowell, B. B.; Flier, J. S.; Maratos-Llier, E. *Nature* **1998**, *396*, 670.
7. Ludwig, D. S.; Tritos, N. A.; Mastaitis, J. W.; Kulkarni, R.; Kokkotou, E.; Elmquist, J.; Lowell, B.; Flier, J. S.; Maratos-Flier, E. *J. Clin. Invest.* **2001**, *107*, 379.
8. Chambers, J.; Ames, R. S.; Bergsma, D.; Muir, A.; Fitzgerald, L. R.; Hervieu, G.; Dytko, G. M.; Foley, J. J.; Liu, W. S. *Nature* **1999**, *400*, 261.
9. Sailer, A. W.; Sano, H.; Zeng, Z.; McDonald, T. P.; Pan, J.; Pong, S. S.; Feighner, S. D.; Tan, C. P.; Fukami, T.; Iwaasa, H. *Proc. Natl. Acad. Sci. U.S.A.* **2001**, *98*, 7564.
10. Forray, C. *Curr. Opin. Pharm.* **2003**, *3*, 85.
11. Kowalski, T. J.; McBriar, M. D. *Ann. Reports Med. Chem.* **2005**, *40*, 119.
12. Dyke, H. J.; Ray, N. C. *Expert Opin. Ther. Patents* **2005**, *15*, 1303.
13. Takekawa, S.; Asami, A.; Ishihara, Y.; Terauchi, J.; Kato, K.; Shimomura, Y.; Mori, M.; Murakoshi, M.; Kato, K.; Suzuki, N.; Nishimura, O.; Fujino, M. *Eur. J. Pharmacol.* **2002**, *438*, 129.
14. Tempest, P.A.; Nixey, T.; Ma, V.; Balow, G.; van Staden, C.; Salon, J.; Rorer, K.; Baumgartner, J.; Hale, C.; Bannon, T.; Hungate, R.; Hulme, C. 227TH National Meeting of the American Chemical Society, Anaheim, CA, 2004; Paper, MEDI298.
15. Handlon, A.L.; Al-Barazanji, K.A.; Barvian, K.K.; Bigham, E.C.; Carlton, D.L.; Carpenter, A.J.; Cooper, J.P.; Daniels, A.J.; Garrison, D.T.; Goetz, A.S.; Green, G.M.; Grizzle, M.K.; Guo, Y.C. Hertzog, D.L.; Hyman, C.E.; Ignar, D.M.; Peckham, G.E.; Speake, J.D.; Britt, C.; Swain, W.R. 228TH National Meeting of the American Chemical Society, Philadelphia, PA 2004; Paper MEDI193.
16. Schwink, L.; Stengelin, S.; Gossel, M.; Bohme, T.; Hessler, G.; Stahl, P.; Gretzke, D. WO 2004/072025.
17. Frimurer, T.M.; Ulven, T.; Hogberg, T.; Norregaard, P.K.; Little, P.B.; Receveur, J.-M. WO 2004/052370.
18. Semple, G.; Kramer, B.; Hsu, D.; Casper, M.; Pleynet, S.S.; Thomsen, B.; Tran, T.A.; Bhenning C.; Whelan, K.; Kanuma, K.; Omodera, K.; Nishiguchi, M.; Funakoshi, T.; Chaki, S.; Sekiguchi, Y. 228TH National Meeting of the American Chemical Society, Philadelphia, PA 2004; Paper MEDI007.
19. Kanuma, K.; Omodera, K.; Nishiguchi, M.; Funakoshi, T.; Chaki, S.; Semple, G.; Tran, T.; Kramer, B.; Hsu, D.; Casper, M.; Thomsen, B.; Sekiguchi, Y. *Bioorg. Med. Chem. Lett.* **2005**, *15*, 3853.
20. Palani, A.; Shapiro, S.; McBriar, M. D.; Clader, J. W.; Greenlee, W. J.; Spar, B.; Kowalski, T. J.; Farley, C.; Cook, J.; van Heek, M.; Weig, B.; O'Neill, K.; Graziano, M.; Hawes, B. *J. Med. Chem.* **2005**, *48*, 4746.
21. Souers, A. J.; Gao, J.; Wodka, D.; Judd, A. S.; Mulhern, M. M.; Napier, J. J.; Brune, M. E.; Bush, E. N.; Brodjian, S. J.; Dayton, B. D.; Shapiro, R.; Hernandez, L. E.; Marsh, K. C.; Sham, H. L.; Collins, C. A.; Kym, P. R. *Bioorg. Med. Chem. Lett.* **2005**, *15*, 2752.
22. Binding assays were determined as described below using mouse, rat or human MCH1 receptors (mMCH-R1, rMCH-R1, and hMCH-R1, respectively) expressed in HEK 293 cells. The assays were performed in 96-well U-bottomed plates. Membranes (100 mg tissue) were incubated at 30 °C for 90 min in assay buffer (25 μM Hepes, 10 μM $MgCl_2$, 0.2% BSA, 0.1 mg/mL soybean trypsin inhibitor, 0.1 mg/mL Pefabloc, and 1μM Phosphoramidon, pH 7.4) with various peptides in the presence of 0.2 nM 125I native-MCH (Perkin-Elmer Life Sciences, Boston, MA) in 100 mL total volume. Non-specific binding was assessed in the presence of 1 μM of cold native-MCH. The reaction was terminated by rapid filtration through Unifilter-96 GF/C glass fiber filter plates (FilterMate® 196 Harvester, Packard Insrument Co., Meriden, CT) pre-soaked in PBS/0.5% BSA, followed by three washes with 300 mL of ice-cold water. Bound radioactivity was determined using a TopCountâ microplate scintillation and luminescence counter (Packard Instrument Co., Meriden, CT). Non-linear regression analyses of drug concentration curves were performed using GraphPad Prism® (GraphPad Software, Inc., San Diego, CA).
23. FLIPR® Protocol (FLIPR® = Fluorometric Imaging Plate Reader): CHOK1-Gqi cells stably expressing MCH-R1 were maintained in Dulbecco's modified Eagle's medium (GICO/Life Technologies, Rockville MD) supplemented with 2 μM glutamine and 10% dialyzed fetal bovine serum

(HyClone, Logan, UT) at 37 °C, 5% CO_2. Cells were harvested, treatment with Versene was followed by trituration, washing twice with cold (4 °C) hybridoma medium (Serum/Protein free, with L-glutamine, sodium bicarbonate, and MOPS buffer) (Sigma–Aldrich Co., St. Louis, MO) and replated onto 96-well black, flat-bottomed, collagen-I coated plates to a density of 10,000 cell/well. The cells were then loaded with the fluorescent calcium indicator Fura-2 (Molecular Probes, Eugene, Or) at 1.6 μM at room temperature. The loaded cells were then washed twice with 90 μL/well of wash buffer. Receptor-stimulated intracellular calcium responses were detected using FLIPR® by monitoring increases in the Fura-2 fluoresence response. Test compounds were screened for MCH-R1 activity in the FLIPR® for both agonist and antagonist action. Agonist mode challenges were conducted at a maximum gradient concentration of 1 μM. Antagonist activity was tested by 10 min pre-incubation of cells at a compound concentration defined to be 300× the EC_{50} of MCH (typically 1 μM), with subsequent introduction of MCH at a concentration 5-fold of EC_{50} as determined in preliminary experiments. Compounds that showed inhibition of MCH induced $MCHR_1$ dependent Ca^{++} responses were automatically tagged for re-interrogation, IC_{50} generation, and Schild analysis. K_i values were calculated from the IC_{50} value according to the Cheng–Prussof equation.

24. Representative procedure: (**i**) To a 2-L glass bottle were added 4-formyl-3-methoxyphenoxy-polystyrene resin **10** (100–180 mesh, 1.1 mmol/g loading, 20 g, 22 mmol, Colorado Biotechnology Associate, Inc.), pyrrolidine ethylamine (5 equiv, 110 mmol, Aldrich), and anhydrous dichloroethane (500 mL, Aldrich). The resulting mixture were shaken for 1 h at room temperature. Then, $Na(OAc)_3BH$ (5 equiv, 110 mmol, Aldrich) was added and the mixture was shaken overnight at room temperature. The mixture was degassed every 30 min for the first three hours. The resin was filtered and washed with methanol (2×) and dichloromethane (2×) to afford **11**; (**ii**) To a 2-L glass bottle were added resin **11**, 4-fluoro-3-nitrobenzoic acid (132 mmol, Aldrich), 1-hydroxybenzotriazole hydrate (132 mmol, Aldrich), diisopropyl carbodiimide (264 mmol, Aldrich), and *N*,*N*-dimethylformamide (500 mL, Aldrich). The resulting mixture was shaken overnight at room temperature. The resin was filtered and washed with *N*,*N*-dimethylformamide (2×), methanol (2×), and dichloromethane (2×) to afford **12**; (**iii**) To a 2-L glass bottle were added resin **12**, 3,4-dimethylphenol (220 mmol, Aldrich), 1,8-diazabicyclo-[5.4.0]undec-7-ene (132 mmol, Aldrich), and *N*,*N*-dimethylformamide (400 mL, Aldrich). The resulting mixture was shaken overnight at room temperature. The resin was filtered and washed with *N*,*N*-dimethylformamide (2×) and dichloromethane (2×) to afford **13**; (**iv**) To a 2-L glass bottle were added resin **13**, tin chloride dihydrate (220 mmol, Aldrich) and *N*,*N*-dimethylformamide (400 mL, Aldrich). The resulting mixture was shaken overnight at room temperature. The resin was filtered and washed with *N*,*N*-dimethylformamide (2×) and dichloromethane (2×) to afford **14**; (**v**) To a peptide vessel were added resin **14** (1.1 mmol/g loading, 100 mg, 0.11 mmol), phenyl isocyanate (1.1 mmol, Aldrich), and 1:1 pyridine: dichloromethane (5 mL, Aldrich). The resulting mixture was shaken overnight at room temperature. The resin was washed with dichloromethane (2×) to afford **15**; (**vi**) A solution of 30% trifluoroacetic acid (Aldrich) in dichloromethane (10 mL) was added to the washed resin and the resulting mixture was shaken for 45 min at room temperature. The resin was filtered and washed with dichloromethane (2×). The combined filtrate was concentrated in vacuo and the residue was purified by silica gel flash chromatography eluting with 30% MeOH/EtOAc to afford compound **27**. ^{1}H NMR (400 MHz, MeOH-d_4): δ 1.38 (m, 2H), 2.01 (m, 3H), 2.27 (s, 6H), 3.16 (m, 5H), 3.68 (t, J = 6.44 Hz, 2H), 6.78 (d, J = 8.55 Hz, 1H), 6.82 (dd, J = 8.28, 2.40 Hz, 1H), 6.91 (br s, 1H), 7.03 (t, J = 7.14 Hz, 1H), 7.19 (d, J = 8.04 Hz, 1H), 7.29 (t, J = 8.04 Hz, 2H), 7.45 (m, 3H), 8.71 (d, J = 2.4 Hz, 1H). ^{13}C NMR (400 MHz, MeOH-d_4): δ 17.74, 18.58, 22.67, 37.03, 54.06, 54.78, 115.57, 116.57, 118.75, 118.93, 120.42, 121.77, 122.54, 128.22, 128.52, 129.89, 130.59, 132.81, 138.49,139.04, 149.79, 153.54, 153.59, 168.97. MS (ESI pos. ion) m/z = 473 $[M+H]^+$. Anal. Calcd for $C_{28}H_{32}N_4O_3 \cdot 0.15CF_3CO_2H \cdot 2.0H_2O$: C, 64.66; H, 6.93; N, 10.66; F, 1.63. Found: C, 64.89; H, 6.79; N, 10.47; F, 1.71.
25. Clark, D. E.; Higgs, C.; Wren, S. P.; Dyke, H. J.; Wong, M.; Norman, D.; Lockey, P. M.; Roach, A. G. *J. Med. Chem.* **2004**, *47*, 3962.
26. Freidinger, R. M. *Curr. Opin. Chem. Biol.* **1999**, *3*, 395.
27. Mason, J. S.; Morize, I.; Menard, P. R.; Cheney, D. L.; Labaudiniere, R.; Hulme, C. *J. Med. Chem.* **1999**, *42*, 3251.
28. Schild experiments were conducted on the FLIPR® for selected compounds by co-administering antagonist compounds together with MC peptide. Several fixed concentrations of antagonist compounds were prepared in 10-fold increments and presented to the cells in a gradient of increasing MCH concentration. Values for pA2 were calculated by linear regression of MCH EC_{50s} as a function of antagonist concentration.
29. In vitro metabolic stability was examined by incubating test compound (1 μM) in rat liver microsomes (0.1 mg/mL) and cofactor NADPH (1 mM) for 0 and 10 min. In addition, incubation without NADPH for 10 min was used to monitor the non-NADPH-dependent degradation. To stop the reaction, equal volume of cold acetonitrile containing internal standard was added to incubate. After vortex and centrifugation at 14000 rpm for 10 min, supernatant was analyzed by LC/MS. The remaining of the test compound was determined by comparing the ratio of the MS response of test compound/internal standard in the 10 min incubates with the presence of NADPH to that in the 0 min incubates. The in vitro intrinsic clearance was calculated based on the rate of metabolism normalized with microsomal protein and incubation time, expressed as μL/min/mg.
30. Male Sprague–Dawley rats (weight range 225–280 g) with surgically implanted femoral vein and jugular vein cannulae were obtained from Hilltop Lab Animals Inc. (Scottsdale, PA). Animals were fasted overnight and the following day compounds were administered either by oral gavage or by intravenous bolus injection. Oral formulations were prepared 24–48 h prior to dosing while intravenous formulations were prepared on the day of dosing. Blood samples were collected over 8 h via jugular cannula into a heparinized tube. Following centrifugation, plasma samples were stored in a freezer to maintain −70 °C until analysis. Lithium heparinized plasma samples (40 μL) were precipitated with acetonitrile containing an internal standard. The supernatant was analyzed by reverse-phase (C-18) LC–MS/MS with atmospheric pressure chemical ionization (APCI) and a Sciex API3000 triple quadrupole mass detector operated in the multiple reaction monitoring (MRM) mode. Study sample concentrations were determined from a weighted ($1/x^2$) linear regression of peak area ratios (analyte peak area/IS peak area) versus the theoretical concentrations of the calibration standards. Pharmacokinetic parameters were calculated by non-compartmental methods using WinNonLin (Pharsight Corporation, Mountainview, CA).